NASA-CR-191270

IN-35

13/6

P-43

Polarization Analysis of a Balloon-Borne Solar Magnetograph

Final Report for

NASA contract NAS8-38609 D.O. 01

Daniel J. Reiley

Russell A. Chipman (PI)

Physics Department

School of Science

University of Alabama in Huntsville

Huntsville, AL 35899

(205)895-6417x318

(NASA-CR-191270) POLARIZATION ANALYSIS OF A BALLOON-BORNE SOLAR MAGNETOGRAPH Final Report (Alabama Univ.) 43 p

N93-16458

Unclas

G3/35 0131699

Table of Contents

Body of the report

The main text of the report contains the particular results of our research which relate directly to the EXVM (Experimental Vector Magnetograph) and the (Balloon-borne Vector Magnetograph) BVM.

I. Polarization 2

A brief overview of which elements in the EXVM and BVM are relevant to this polarization analysis.

II. Polarization Specification 2

A qualitative discussion of the possible meaning of the 10^{-5} polarization specification for the BVM. A recommendation of which polarization specification is most relevant for the BVM. A diattenuation budget for the various surfaces in the BVM which will allow the polarization specification to be met.

III. Specifying the Coatings 5

An explanation of the various coating specifications which are recommended.

IV. Optical Design of the EXVM 8

V. Coating specification sheets for the BVM 22

Appendices

The appendices of this report contain the more general results of our research on the general topic of polarization aberrations.

Appendix I. 27

A general discussion of polarization aberration theory, in terms of the SAMEX solar magnetograph,

Appendix II. 28

Rigorous derivations for the Mueller matrices of optical systems.

I. Polarization

The mirrors and lenses in optical systems can change light's polarization state. Since solar magnetographs operate by measuring the polarization state of the solar disc, the effect of the mirrors and lenses on the polarization state must be well-characterized.

One way to characterize mirrors' and lenses polarization properties is to use polarization aberration theory. Polarization aberration theory is applied to a previous solar magnetograph design in the paper "Polarization analysis of the SAMEX solar magnetograph," which is included in this report as Appendix I.

Since the polarimeter used in this system will be a rotating-retarder polarimeter, the polarization state exiting the polarimeter will be constant. Therefore, the only optical elements which will affect the accuracy of the Solar magnetic field measurements will be the polarization that is caused be the optics in front of the polarimeter.

II. Polarization specification

The polarization for this system was specified to be below 10^{-5}. This specification can have several meanings in terms of the polarization aberration coefficients that are associated with the system. These errors are derived in Appendix II, and are only summarized in this section.

We have enumerated three polarization errors which are possible in the solar magnetograph:

Polarization Error #1: The first polarization error is that unpolarized light can couple into polarized light. The first effect of this polarization error is that magnetic field is measured

when no magnetic field is present. The second effect of this polarization error is that the orientation of linearly polarized light is measured incorrectly, causing the orientation of the magnetic field to be measured incorrectly. The symptom of this polarization error is a spurious, radially oriented linear polarization with magnitude that increases quadratically with field coordinate. Mathematically, this polarization error is $2 \mid Re(P_{1200}) \mid < 10^{-5}$. For the BVM with an articulating secondary mirror and the coatings specified in Section V, the value for this polarization error is $2 \mid Re(P_{1200}) \mid < .9@.10^{-5}$. Since this value depends only on the chief ray, this value is the same for either the 60 cm telescope or the 30 cm. telescope.

Polarization Error #2: The second polarization error is that polarized light couples into the wrong polarization state. The first effect of this polarization error is that the orientation of linearly polarized light is measured incorrectly, causing the orientation of the magnetic field to be measured incorrectly. The second effect of this polarization error is an error in the measured degree of linear polarization, also causing the orientation of the magnetic field to be measured incorrectly. The magnitude of this polarization error is $2 \mid P_{1200} \mid < 10^{-5}$. For the BVM with an articulating secondary mirror and the coatings specified in Section V, the value for this polarization error is $2 \mid Re(P_{1200}) \mid < \sim 1.8 \cdot 10^{-5}$. The value is approximate because the specifications in Section V are for diattenuation only. Since this value depends only on the chief ray, this value is the same for either the 60 cm telescope or the 30 cm. telescope.

Polarization Error #3: The third polarization error is that polarized light couples into unpolarized light. The effect of this polarization error is that the magnitude of the measured field is underestimated, raising the threshold of the measurable magnetic field. The magnitude of this polarization error is represented by the magnitude of all the polarization aberration coefficients. For the BVM with an articulating secondary mirror, a 30 cm. telescope, and the coatings specified in Section V, the value for this polarization

error is $D < \sim 3 \cdot 10^{-8}$. The value is approximate because the specifications in Section V are for diattenuation along the chief ray only. This value is approximately quadratic in f-number, so the value for a 60 cm. telescope is $D < \sim 12 \cdot 10^{-8}$.

We believe that polarization error #1 is the most relevant to this problem. The 10^{-5} polarization specification would then require that $2ReP_{1200} < 10^{-5}$.

The polarization aberration coefficients depend on the angles of incidence for the chief and marginal rays as well as the coatings on the various surfaces. With a tilted secondary mirror, the angles of incidence on the relevant surfaces are listed in Table 1.

Table 1

Angles of Incidence

(with secondary tilted .3°)

	marginal ray	chief ray
prefilter	0°	.16°
primary mirror	3.6°	.16°
secondary mirror	4.5°	.3°
front surface of lens	2.3°	2.2°
inner surface of lens	9.3°	4.7°
back surface of lens	6.5°	3.2°

Polarization tilt diattenuation is small even with no coatings on any of the surfaces, $ReP_{1200} = 8.3 \cdot 10^{-5}$. The distribution of polarization diattenuation piston when the surfaces are uncoated are listed in Table 2.

Table 2

Polarization Piston Diattenuation

all surfaces uncoated

(with secondary tilted .3°

Surface	$Re\,P_{1200}$
Primary mirror	$-.05\cdot 10^{-5}$
Secondary mirror tilted .15°	$-.05\cdot 10^{-5}$
front surface of lens	$1.6\cdot 10^{-5}$
inner surface of lens	$.8\cdot 10^{-5}$
back surface of lens	$6\cdot 10^{-5}$
SUM	$8.3\cdot 10^{-5}$

The negative sign on the coefficients in Table 2 for the mirrors indicates that the elements are used in reflection rather than transmission. The .3° tilt on the secondary mirror corresponds to a 10 arcminute change in the center of the field of view.

The values in Table 2 were calculated using the following equation:

$$R_p(\theta_{c,t}) - R_s(\theta_{c,t}) = r_p^2 - r_s^2$$

$$= (1-\eta_p)^2 - (1-\eta_s)^2$$

$$\cong 2(\eta_s - \eta_p)$$

$$= 2(r_s(\theta_{c,t}) - r_p(\theta_{c,t}))$$

$$= 2Re(P_{1200}),$$

where R_s and R_p are the s- and p- intensity reflection coefficients, r_s and r_p are the s- and p- amplitude reflection coefficients, η_s and η_p are the small deviations of r_s and r_p from one, and $\theta_{c,i}$ is the chief ray angle of incidence on surface i.

III. Specifying the coatings

The coatings should be specified so that the diattenuation along the chief ray path is less than 10^{-5}. We suggest the following diattenuation budget listed in Table 3.

Prefilter

$0 < R_p - R_s < .1\,10^{-5}$ $\quad 0° < \theta < .16°$

Primary mirror

$.05\,10^{-5} < R_p - R_s < .5\,10^{-5}$ $\quad 0° < \theta < .16°$

Secondary mirror

$.05\,10^{-5} < R_p - R_s < .5\,10^{-5}$ $\quad 0° < \theta < .18°$

Doublet (front)

$0 < R_p - R_s < .1\,10^{-5}$ $\quad 0° < \theta < .8°$

Doublet (internal surface)

$R_p - R_s = 1.5\,10^{-5}$ (fixed)

Doublet (back)

$0 < R_p - R_s < .1\,10^{-5}$ $\quad 0° < \theta < 3.3°$

This diattenuation budget will give a polarization aberration of $2Re(P_{1200}) < .9 \cdot 10^{-5}$. We also suggest that the mirrors have high reflectivity, > 98% over the entire range of relevant incident angles and apertures.

Several characteristics of this diattenuation budget may not be immediately obvious. The first characteristic is that the diattenuation of the internal surface of the doublet is the limiting factor. To balance the diattenuation of the internal surface of the doublet, we place upper and lower bounds on the diattenuation of the telescope mirrors. Although the specified differences in reflectivity are all of the same sign, the diattenuations balance because the prefilter and the lens are used in transmission. The antireflection coating on the back side of the doublet will be the hardest to make because of the relatively large angles of incidence on that surface.

Notice that no coatings are required if the polarimeter is placed in front of the first doublet.

Since the required diattenuation values are close to the diattenuation values for the

uncoated interfaces, coating vendors should have little problem designing economical coatings which meet this specification. We choose not to provide coating designs with this report because the most economical way to meet these specifications varies widely from vendor to vendor. Most vendors have stock coating designs which will meet these specifications, and will not charge for coating design.

A more serious problem than devising coating designs which meet this polarization specification is the problem of verifying that these specifications were actually met. These low polarization coatings would require very precise ellipsometry to verify that the polarization specifications are met. One possible way to accomplish this is to take advantage of the fact that diattenuation is quadratic in angle of incidence. This quadratic behavior is what determines the polarization specification for the 45° angle of incidence on the coating specification sheets in Appendix IV. Simpler, less precise, ellipsometric techniques can be used to find the relatively large diattenuation at the large angle of incidence.

The coatings should be specified to degrade the surface figure by less than $\lambda/10$ RMS over the entire clear aperture, to prevent degradation of image quality. Surface quality should be specified to meet MIL-SPEC 60-40 scratch-dig specifications; this is a typical surface quality specification for scientific-grade optics. Surface durability should be specified to meet the MIL-SPEC scotch tape test and eraser test; this is a fairly stringent requirement, which we feel is justified because this instrument will be used outdoors.

Although the polarization specifications for these coatings are for the real part of polarization piston, we can use them to estimate what the other aberration terms would be, and therefore estimate the magnitude of other polarization errors. First, since we know the angles of incidence for the marginal ray, and since we have specified the diattenuation for the chief ray, we can use the quadratic behavior of diattenuation to estimate the real parts of polarization tilt, $Re(P_{1111})$, and polarization defocus, $Re(P_{1022})$. Since, for many

coatings, the imaginary parts of the polarization aberration coefficients are close to the real parts, $Re(P_{xxxx}) \cong Im(P_{xxxx})$, we can estimate the other polarization effects.

One effect of polarization error #2 listed above is the coupling of circular polarization states into linear ones. This coupling is represented by the M_{43} element of the matrix in eq. 2 of Appendix II.

$M_{43} = 2h^2 P_{0000} q_{1200}$

For radially symmetric systems, this term is simply a quadratic term from the center of the pupil to the edge of the pupil. For tilted and decentered systems, this quadratic variation is moved from the center of the field to another point in the field. This coupling term is plotted in Figures 3 & 4. For a magnetograph with a tilting secondary mirror and the coatings outlined above, the magnitude of this error should be $M_{43} < .9\,10^{-5}$. This value was calculated by assuming the transmission of the system is close to one, $P_{0000} \cong 1$, and the real part of polarization piston is about equal to the imaginary part of polarization piston, $Re(P_{1022}) \cong Im(P_{1022})$.

Polarization error #3 can also be estimated. The depolarization of the system is estimated in Appendix III to be

$D = \frac{1}{3} P_{1022}^2 + \frac{1}{2} h^2 P_{1111}^2$.

Assuming a quadratic variation in diattenuation and retardance on each surface, and assuming that the real and imaginary parts of the polarization aberrations are equal, the magnitude of polarization piston will be

$|P_{1111}| \cong 1.4 \cdot 10^{-5}$,

and the magnitude of polarization defocus will be

$|P_{1111}| \cong 29 \cdot 10^{-5}$.

The depolarization of the system will then be $D \cong 3 \cdot 10^{-8}$. This is the maximum depolarization at the edge of the field of view for a system with a tilted secondary mirror.

The following two pages describe the polarization errors graphically.

Diattenuation Vectors

In the image plane, the main polarization defect introduced by the coatings is the diattenuation caused by the real part of P1200

Foa a centered system (no tilted secondary), the diattenuation vectors are radially oriented in the image plane, with quadratically increasing amplitude..
For the specified coatings, the magnitude of the largest line shown here is .7E-5.

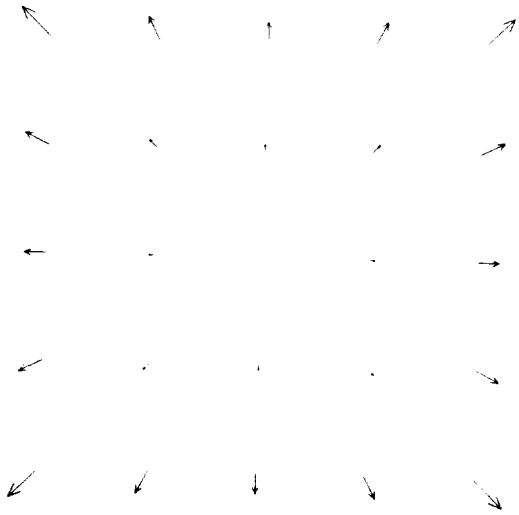

For a tilted secondary, the diattenuation vectors have the same pattern, but are not centered in the center of the field. The exact location of the center depends on the coatings and amouont of tilt, but this figure is reasonable.
For the specified coatings, the magnitude of the largest line shown here is 1E-5.

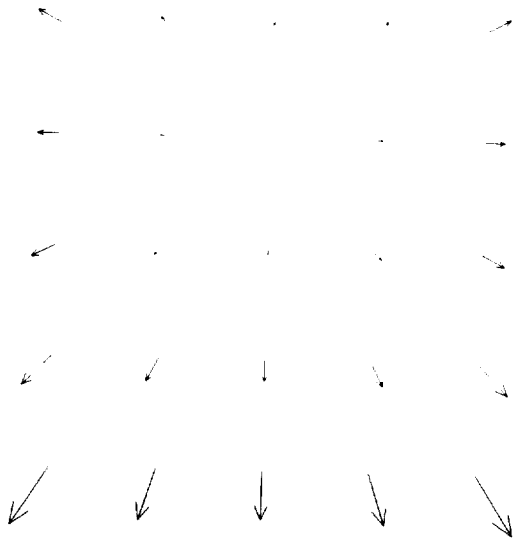

■ **Effect of retardance along the chief ray**

In the image plane, the next most important effect of polarization aberrations is the

retardance caused by the imaginary part of P1200. These values will have the same orientation and approximately the same values as the diattenuation plots shown above

Effect of other polarization aberrations

In the image plane, the effect of the other polarization aberrations is depolarization. For a radially symmetric system, this depolarization increases quadratically from the center of the field of view.

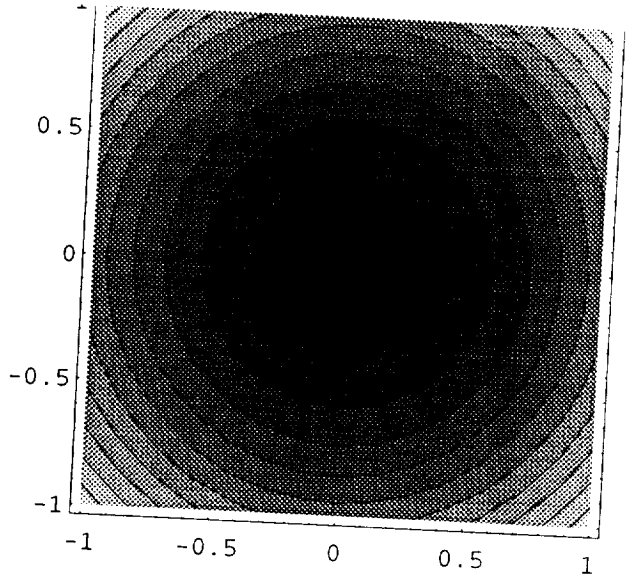

With a tilted secondary, this depolarization increases quadratically from some other point in the field of view.

The plot shown here is rotated 90 degrees with respect to the diattenuation plots.

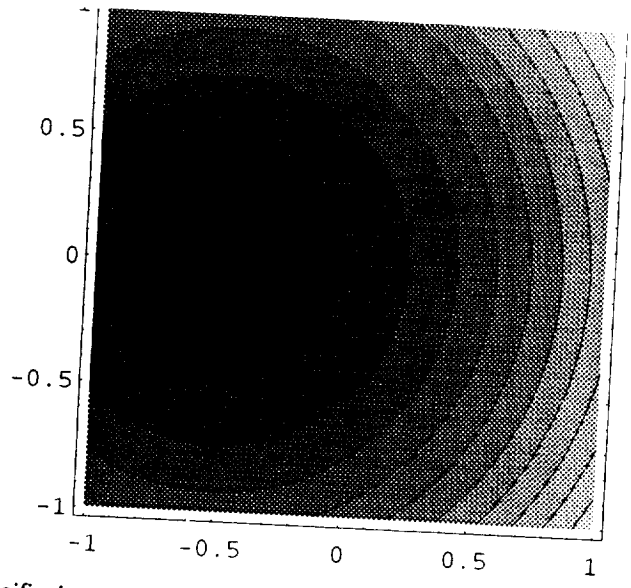

For the specified coatings, the maximum contour line shown here would be less than 3E-8.

IV. Optical design of the EXVM

While working on the polarization analysis of the NASA-designed instrument, we noticed that it could be fabricated much more economically if catalog lenses were used instead of custom lenses. After discussing the possibility with Mona Hagyard, Alan Gary, and Ed West of NASA, we decided to redesign the optical system to take advantage of these lenses.

Catalog lenses are lenses which are made for common optical tasks such as collimating and focussing laser beams. Companies such as Melles-Griot, Spindler & Hoyer, JML, Newport, Edmund, and CVI have dedicated large amounts of capital to produce large numbers of commonly-requested focal lengths and diameters. Because these lenses are made on a regular basis, they are much less expensive than custom lenses of similar quality.

Table 4 lists the optical prescription for this system. Each of the lenses is a catalog lens. Figure 1 is a schematic of the system.

Table 4

Optical prescription for the EXVM

	RDY	THI	GLA	Clear Aperture
> OBJ:	INFINITY	INFINITY		
1:	INFINITY	0.001000	BK7_SCHOTT	306.653
2:	INFINITY	650.000000		306.653
STO:	-2394.73740	-877.239800	REFL	304.8
	K: -1.000000			
4:	-858.24060	1069.000000	REFL	83.9923
	K: -2.82538			
5:	INFINITY	7.000000	BK7_SCHOTT	24.1539
6:	INFINITY	5.000000		23.8961
7:	INFINITY	50.000000	BK7_SCHOTT	23.6162
8:	INFINITY	5.000000		21.7747
9:	INFINITY	6.000000	BK7_SCHOTT	21.4949
10:	INFINITY	5.000000		21.2739
11:	INFINITY	7.000000	BK7_SCHOTT	20.994
12:	INFINITY	5.000000		20.7362
13:	INFINITY	3.000000	BK7_SCHOTT	20.4563
14:	INFINITY	315.000000		20.3458
15:	718.39000	4.000000	SF8_SCHOTT	27.4918
16:	92.73000	6.600000	SSK4_SCHOTT	27.6017
17:	-128.08000	105.000000		27.8829

18:	INFINITY	300.000000		
19:	INFINITY	33.500000	BK7_SCHOTT	20.9224
20:	210.75000	5.000000		18.1876
21:	-81.29000	4.400000	BAK4_SCHOTT	20.4624
22:	-515.63000	75.000000	F3_SCHOTT	20.5015
23:	INFINITY	-128.880000		20.5668
	ADE: 45		REFL	20.5172
24:	141.25000	-4.800000	SF5_SCHOTT	20.4319
25:	47.31500	-3.000000	BK7_SCHOTT	20.7112
26:	-61.74800	-15.000000		20.7653
27:	INFINITY	0.010000	BK7_SCHOTT	23.7989
28:	INFINITY	-48.000000		23.7975
29:	INFINITY	-4.000000	BK7_SCHOTT	33.5049
30:	INFINITY	-48.000000		34.0372
31:	INFINITY	0.010000	BK7_SCHOTT	43.7446
32:	INFINITY	-112.017000		43.7432
33:	-188.36000	-12.500000	BK7_SCHOTT	66.3972
34:	139.24000	-6.000000	SF5_SCHOTT	66.5534
35:	415.67000	-55.000000		66.8955
36:	INFINITY	165.233309	REFL	66.142
	ADE: 45			
37:	INFINITY	4.000000	BK7_SCHOTT	63.8781
38:	INFINITY	12.000000		63.842
39:	INFINITY	21.000000	BK7_SCHOTT	63.6776
40:	INFINITY	0.000275		63.713
41:	INFINITY	18.000000	BK7_SCHOTT	63.713
42:	INFINITY	0.000000		63.8744
43:	INFINITY	21.000000	BK7_SCHOTT	63.8744
44:	INFINITY	12.000000		64.0626
45:	INFINITY	4.000000	BK7_SCHOTT	64.2261
46:	INFINITY	80.000000		64.2619
47:	673.17000	6.000000	SF5_SCHOTT	65.3518
48:	222.27000	10.000000	BK7_SCHOTT	65.1645
49:	-302.87000	439.000000		65.1296
50:	121.71195	3.800000	BK7_SCHOTT	13.7199
51:	-89.71796	2.500000	SF5_SCHOTT	13.2806
52:	-268.15906	131.029506		13.0547
53:	32.16000	4.460000	SK11_SCHOTT	17.9977
54:	-22.47000	1.500000	SF5_SCHOTT	17.4991
55:	-89.36000	34.925611		17.4214
56:	INFINITY	-120.845313	REFL	9.74839
	ADE: -15			
57:	-182.72000	-2.000000	SF5_SCHOTT	16.8009
58:	-44.88000	-4.800000	SK11_SCHOTT	16.9879
59:	64.04000	-72.000000		17.6003
60:	INFINITY	257.078523	REFL	20.7726
	ADE: 15			
61:	INFINITY	-72.000000	REFL	32.0994
	ADE: 45			
62:	INFINITY	108.000000	REFL	35.2717
	ADE: -45			
IMG:	INFINITY	0.000000		40.0302

SPECIFICATION DATA

EPD	304.80000		
DIM	MM		
WL	656.27	632.80	525.02
YAN	0.00000	0.05717	0.08167

REFRACTIVE INDICES			
GLASS CODE	656.27	632.80	525.02
SSK4 SCHOTT	1.614266	1.615305	1.621923
SF8 SCHOTT	1.682505	1.684452	1.697362
BAK4 SCHOTT	1.565761	1.566704	1.572695
F3 SCHOTT	1.608063	1.609545	1.619244
BK7 SCHOTT	1.514323	1.515089	1.519867
SF5 SCHOTT	1.666612	1.668457	1.680666
SK11 SCHOTT	1.561011	1.561883	1.567374

INFINITE CONJUGATES

EFL	-14063.1395
BFL	109.3923
FFL	-0.3236E+06
FNO	-46.1389
IMG DIS	108.0000
OAL	2301.9661

PARAXIAL IMAGE

HT	20.0458
ANG	0.0817

EXIT PUPIL

DIA	13.2190
THI	-500.5187

Figure 1: Schematic of the EXVM

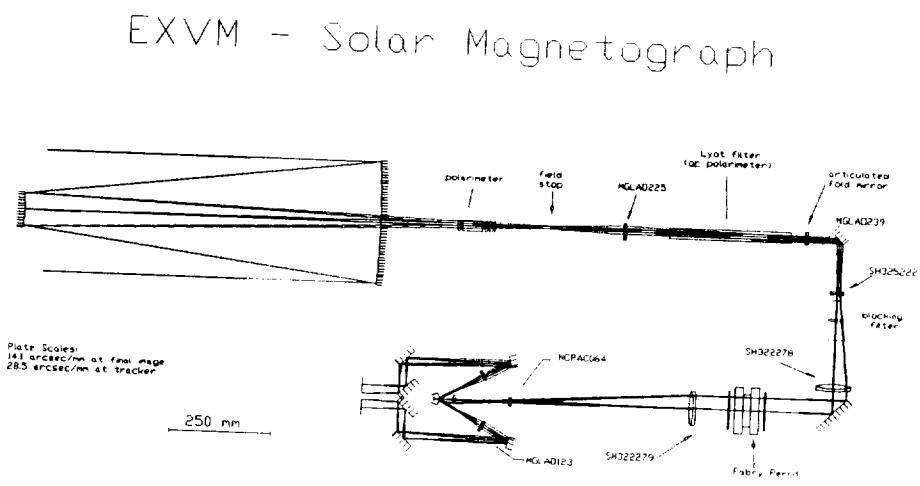

Table 5 lists the first-order properties of the system. HMY is the height of the marginal ray, UMY is the slope of the marginal ray, HCY is the height of the chief ray, and UCY is the slope of the chief ray. A second representation of the system's first-order properties is in Figure 2, the y-y bar diagram of the system.

Table 5

First-Order properties of the EXVM system

	HMY	UMY	HCY	UCY
EP	152.400000	0.000000	0.000000	0.001425
1	152.400000	0.000000	-0.926518	0.000938
2	152.400000	0.000000	-0.926517	0.001425
STO	152.400000	0.127279	0.000000	-0.001425
4	40.745715	-0.032327	1.250428	0.004339
5	6.187768	-0.021270	5.889186	0.002855
6	6.038879	-0.032327	5.909172	0.004339
7	5.877242	-0.021270	5.930868	0.002855
8	4.813749	-0.032327	6.073623	0.004339
9	4.652112	-0.021270	6.095319	0.002855
10	4.524493	-0.032327	6.112450	0.004339
11	4.362856	-0.021270	6.134146	0.002855
12	4.213967	-0.032327	6.154132	0.004339
13	4.052330	-0.021270	6.175829	0.002855
14	3.988520	-0.032327	6.184394	0.004339
15	-6.194598	-0.015503	7.551287	-0.001762
16	-6.256610	-0.019362	7.544239	0.001940
17	-6.384400	-0.000403	7.557043	-0.033548
18	-6.426724	-0.000265	4.034458	-0.022073
19	-6.506285	-0.000403	-2.587524	-0.033548
20	-6.519789	0.011009	-3.711396	-0.014919
21	-6.464743	0.008406	-3.785991	-0.015829
22	-6.427755	0.021331	-3.855639	-0.021001
23	-4.827902	-0.021331	-5.430683	0.021001
24	-2.078715	-0.006732	-8.137238	0.035827
25	-2.046401	-0.012020	-8.309207	0.021038
26	-2.010341	-0.001344	-8.372319	0.102462
27	-1.990187	-0.000884	-9.909252	0.067415
28	-1.990196	-0.001344	-9.908578	0.102462
29	-1.925704	-0.000884	-14.826762	0.067415
30	-1.922168	-0.001344	-15.096423	0.102462
31	-1.857677	-0.000884	-20.014606	0.067415
32	-1.857685	-0.001344	-20.013932	0.102462
33	-1.707182	-0.003984	-31.491437	0.010229
34	-1.657381	-0.002464	-31.619301	0.030977
35	-1.642596	-0.006831	-31.805163	-0.000019
36	-1.266885	0.006831	-31.804096	0.000019
37	-0.138158	0.004495	-31.800888	0.000013
38	-0.120180	0.006831	-31.800837	0.000019
39	-0.038206	0.004495	-31.800604	0.000013
40	0.056179	0.006831	-31.800336	0.000019
41	0.056181	0.004495	-31.800336	0.000013
42	0.137083	0.006831	-31.800106	0.000019
43	0.137083	0.004495	-31.800106	0.000013
44	0.231468	0.006831	-31.799838	0.000019
45	0.313442	0.004495	-31.799605	0.000013
46	0.331420	0.006831	-31.799554	0.000019
47	0.877909	0.003536	-31.798001	0.019142
48	0.899127	0.004338	-31.683148	0.006086
49	0.942511	0.004976	-31.622283	0.063529

50	3.127019	-0.005514	-3.732943	0.052290
51	3.106067	-0.001674	-3.534241	0.043518
52	3.101882	-0.010687	-3.425446	0.081834
53	1.701589	-0.025971	7.297245	-0.029926
54	1.585757	-0.019463	7.163775	-0.006418
55	1.556562	-0.044568	7.154148	-0.065280
56	0.000000	0.044568	4.874194	0.065280
57	-5.385824	0.014580	-3.014621	0.032160
58	-5.414985	0.024355	-3.078942	0.039443
59	-5.531890	-0.010837	-3.268270	0.032867
60	-4.751638	0.010837	-5.634672	-0.032867
61	-1.965719	-0.010837	-14.083994	0.032867
62	-1.185466	0.010837	-16.450397	-0.032867
IMG	-0.015088	0.010837	-20.000000	-0.032867

Figure 2: y- y bar diagram of the EXVM.

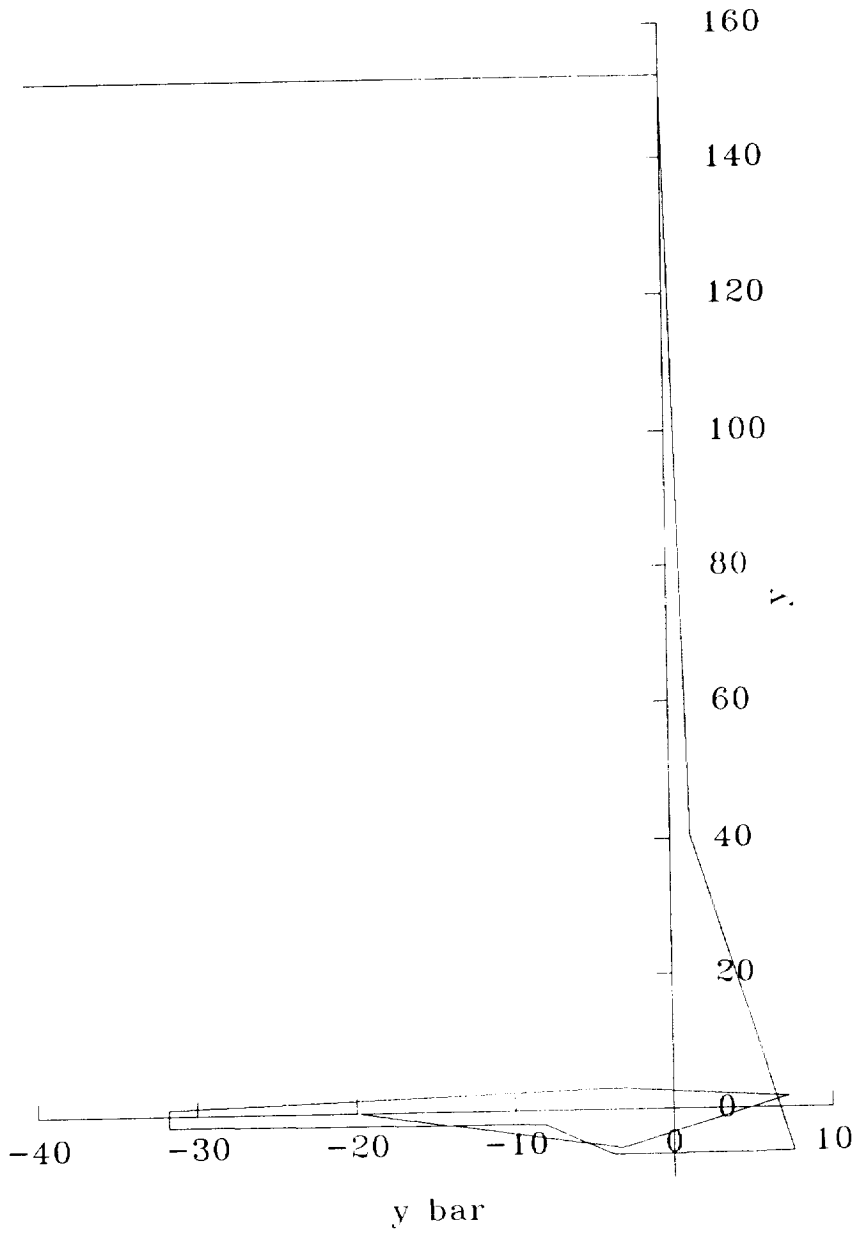

Table 6 lists the surface-by-surface third-order aberrations of the EXVM. SA stand for spherical aberration, TCO stands for tangential coma, TAS stands for tangential astigmatism, SAG stands for saggital astigmatism, PTB stands for Petzval blur, and DST stands for distortion. All aberrations are in millimeters.

Table 6

Third-order aberrations of the EXVM

	SA	TCO	TAS	SAG	PTB	DST
1	0.000000	0.000000	0.000000	0.000000	0.000000	0.000012
2	0.000000	0.000000	0.000000	0.000000	0.000000	-0.000012
STO	3.624628	-0.243555	0.003637	0.000000	-0.001818	0.000000
	-3.624628	0.000000	0.000000	0.000000		0.000000
4	-1.136824	0.123181	0.000625	0.003591	0.005074	-0.000130
	1.136776	0.104658	0.003212	0.001071		0.000033
5	-0.005470	0.002203	-0.000296	-0.000099	0.000000	0.000013
6	0.005338	-0.002150	0.000289	0.000096	0.000000	-0.000013
7	-0.005195	0.002092	-0.000281	-0.000094	0.000000	0.000013
8	0.004255	-0.001714	0.000230	0.000077	0.000000	-0.000010
9	-0.004112	0.001656	-0.000222	-0.000074	0.000000	0.000010
10	0.004000	-0.001611	0.000216	0.000072	0.000000	-0.000010
11	-0.003857	0.001553	-0.000208	-0.000069	0.000000	0.000009
12	0.003725	-0.001500	0.000201	0.000067	0.000000	-0.000009
13	-0.003582	0.001443	-0.000194	-0.000065	0.000000	0.000009
14	0.003526	-0.001420	0.000191	0.000064	0.000000	-0.000009
15	0.011116	-0.012094	0.005631	0.002707	0.001245	-0.000982
16	-0.016057	0.046209	-0.044970	-0.015419	-0.000643	0.014791
17	0.008307	-0.046646	0.093831	0.035623	0.006518	-0.066680
18	0.000000	0.000003	0.000229	0.000076	0.000000	0.006349
19	0.000000	-0.000003	-0.000232	-0.000077	0.000000	-0.006428
20	0.002187	0.010711	0.021248	0.009591	0.003762	0.015656
21	-0.010937	-0.011472	-0.004501	-0.001827	-0.000490	-0.000639
22	0.005467	-0.006563	0.004241	0.002490	0.001615	-0.000996
23	0.000000	0.000000	0.000000	0.000000	0.000000	0.000000
24	-0.002159	-0.006579	-0.012924	-0.008470	-0.006243	-0.008601
25	0.002601	0.021819	0.063919	0.023238	0.002897	0.064989
26	-0.000593	-0.013574	-0.115584	-0.046569	-0.012061	-0.355156
27	0.000000	0.000029	-0.002204	-0.000735	0.000000	0.056016
28	0.000000	-0.000029	0.002204	0.000735	0.000000	-0.056016
29	0.000000	0.000028	-0.002132	-0.000711	0.000000	0.054201
30	0.000000	-0.000028	0.002128	0.000709	0.000000	-0.054101
31	0.000000	0.000027	-0.002057	-0.000686	0.000000	0.052286
32	0.000000	-0.000027	0.002057	0.000686	0.000000	-0.052286
33	0.000006	0.000629	0.025908	0.011272	0.003954	0.393726
34	-0.000052	-0.002109	-0.029773	-0.010581	-0.000984	-0.144424
35	0.000047	0.001007	0.009266	0.004503	0.002121	0.031962
36	0.000000	0.000000	0.000000	0.000000	0.000000	0.000000
37	-0.000001	0.000000	0.000000	0.000000	0.000000	0.000000
38	0.000001	0.000000	0.000000	0.000000	0.000000	0.000000
39	0.000000	0.000000	0.000000	0.000000	0.000000	0.000000
40	0.000000	0.000000	0.000000	0.000000	0.000000	0.000000
41	0.000000	0.000000	0.000000	0.000000	0.000000	0.000000
42	-0.000001	0.000000	0.000000	0.000000	0.000000	0.000000
43	0.000001	0.000000	0.000000	0.000000	0.000000	0.000000
44	-0.000002	0.000000	0.000000	0.000000	0.000000	0.000000
45	0.000003	0.000000	0.000000	0.000000	0.000000	0.000000
46	-0.000003	0.000000	0.000000	0.000000	0.000000	0.000000
47	0.000013	-0.000221	0.002591	0.001737	0.001310	-0.010080
48	-0.000005	0.000247	-0.004633	-0.001956	-0.000617	0.031830

49	0.000000	-0.000087	-0.005347	-0.000143	0.002459	-0.012892
50	0.001168	0.003753	0.010140	0.007459	0.006119	0.007992
51	-0.001403	0.009618	-0.023498	-0.008851	-0.001528	0.020220
52	0.000687	-0.008760	0.040530	0.015702	0.003288	-0.066755
53	0.000823	0.018063	0.156585	0.068533	0.024507	0.501119
54	-0.008358	-0.090578	-0.331361	-0.113232	-0.004167	-0.409025
55	0.009103	0.064030	0.159999	0.059912	0.009868	0.140474
56	0.000000	0.000000	0.000000	0.000000	0.000000	0.000000
57	0.048899	0.162022	0.183774	0.064475	0.004826	0.071211
58	-0.088585	-0.198013	-0.149627	-0.051266	-0.002086	-0.038199
59	0.063628	0.035672	0.018974	0.014529	0.012307	0.002715
60	0.000000	0.000000	0.000000	0.000000	0.000000	0.000000
61	0.000000	0.000000	0.000000	0.000000	0.000000	0.000000
62	0.000000	0.000000	0.000000	0.000000	0.000000	0.000000
SUM	0.024479	-0.038080	0.081811	0.068093	0.061233	0.182185

Figure 3: Wavefront aberrations of the EXVM in the final image plane.

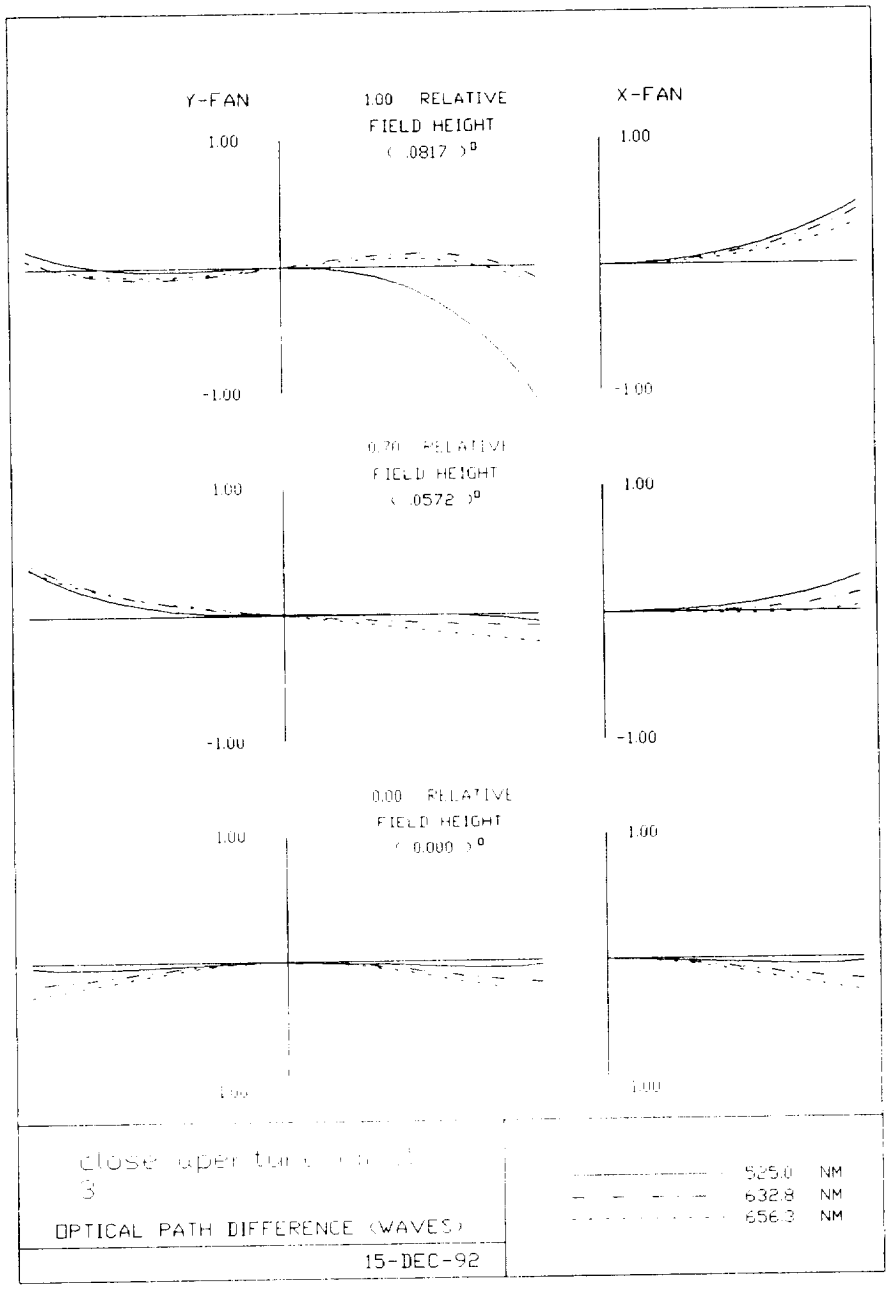

REILEY

10:03:01

Section V - Coating specification sheets

Prefilter

diagram of blank

Average intensity transmittance

> __% over entire diameter, incident angles 0° - .16°

λ = 525nm

< __% outside of __ nm bandpass, centered on λ = 525nm

over entire diameter, incident angles 0° - .16°

Polarization

R_s - s-polarization intensity reflectivity

R_p - p-polarization intensity reflectivity

$0 < R_p - R_s < .1 \cdot 10^{-5}$

over entire clear aperture, incident angles 0° - .16°

λ = 525nm

Surface figure

surface figure must be degraded less than λ /10 at λ = 633 nm

Surface quality

must meet MIL-SPEC 60-40 scratch-dig specification over entire surface

Surface durability

must meet MIL-SPEC scotch tape and eraser tests

Primary mirror

diagram of mirror

Average intensity reflectivity

>98% over entire diameter, incident angles 0° - 3.8°

λ = 525nm

Polarization

R_s - s-polarization intensity reflectivity

R_p - p-polarization intensity reflectivity

$.05 \cdot 10^{-5} < R_s - R_p < .5 \cdot 10^{-5}$

over entire clear aperture, incident angles 0° - .16°

λ = 525nm

$.04 < R_p - R_s < .4$ for incident angle = 45°

λ = 525nm

Surface figure

surface figure must be degraded less than $\lambda/10$ at λ = 633 nm

Surface quality

must meet MIL-SPEC 60-40 scratch-dig specification over entire surface

Surface durability

must meet MIL-SPEC scotch tape and eraser tests

Secondary mirror

diagram of mirror

Average intensity reflectivity

>98% over entire diameter, incident angles 0° - 4.6°
λ = 525nm

Polarization

R_s - s-polarization intensity reflectivity
R_p - p-polarization intensity reflectivity

$.05 \cdot 10^{-5} < R_s - R_p < .5 \cdot 10^{-5}$
over entire clear aperture, incident angles 0° - .8°
λ = 525nm

$R_s - R_p <$ __ for incident angle = 45°
λ = 525nm

Surface figure

surface figure must be degraded less than $\lambda/10$ at λ = 633 nm

Surface quality

must meet MIL-SPEC 60-40 scratch-dig specification over entire surface

Surface durability

must meet MIL-SPEC scotch tape and eraser tests

Front doublet surface

diagram of lens

Average intensity transmittance
<98% over entire diameter, incident angles 0° - __°
λ = 525nm

Polarization
R_s - s-polarization intensity reflectivity
R_p - p-polarization intensity reflectivity

$0 < R_p - R_s < .1 \cdot 10^{-5}$
over entire clear aperture, incident angles 0° - .8°
λ = 525nm

$R_s - R_p < .03$ for incident angle = 45°
λ = 525nm

Surface figure
surface figure must be degraded less than $\lambda/10$ at λ = 633 nm

Surface quality
must meet MIL-SPEC 60-40 scratch-dig specification over entire surface

Surface durability
must meet MIL-SPEC scotch tape and eraser tests

Back doublet surface

diagram of lens

Average intensity transmittance

>98% over entire diameter, incident angles 0° - 5.1°

λ = 525nm

Polarization

R_s - s-polarization intensity reflectivity

R_p - p-polarization intensity reflectivity

$0 < R_p - R_s < .1 \cdot 10^{-5}$

over entire clear aperture, incident angles 0° - 3.3°

λ = 525nm

$R_s - R_p < 2 \cdot 10^{-4}$ for incident angle = 45°

λ = 525nm

Surface figure

surface figure must be degraded less than $\lambda/10$ at λ = 633 nm

Surface quality

must meet MIL-SPEC 60-40 scratch-dig specification over entire surface

Surface durability

must meet MIL-SPEC scotch tape and eraser tests

Appendix I. The paper "Polarization Analysis of the SAMEX Solar Magnetograph" contains both a good summary of polarization aberration theory and a good demonstration of polarization aberration analysis.

Appendix II. Polarization Aberrations of unresolved point spread functions

This section explicitly provides the mathematics behind the polarization specification which was presented in Section III. First, we present the reasoning for the derivation of the Mueller matrix averaged over the point spread function. Next, we derive the average Mueller matrix for rotationally symmetric systems. Then, we use this Mueller matrix to explore the three possible explanations of the 10^{-5} polarization specification in rotationally symmetric systems. Finally, we explain how the result from rotationally symmetric systems can be generalized into a result for slightly decentered systems, such as a vector magnetograph with an actuating secondary mirror.

In many imaging situations, the point spread function that is formed by the system's optics is smaller than the resolution of the system's readout. The EXVM is a good example of this type of system; the pixels on the CCD array are slightly larger than the point spread function.

For this situation, the Stokes vector averaged over the point spread function is equal to the pupil-averaged Stokes vector. This equality can be understood by recognizing that the intensity in the pupil of any two orthogonal polarization states is the same as the intensity of those polarization states in the image. For example, if a 90% of the intensity in the pupil is y-polarized and 10% is x-polarized, the intensity distribution in the image plane will also be 90% y-polarized and 10% x-polarized. Just as the polarization state changes across the pupil, the polarization state will also change across the point spread function, but the average Stokes vector will be the same.

This equality can also be derived. The Jones vector in the exit pupil is

$$\vec{E} = \begin{pmatrix} E_x \\ E_y \end{pmatrix}.$$

The Stokes vector in the exit pupil is defined in terms of sums and differences in intensity measurements,

$$\vec{S} = \begin{pmatrix} I \\ Q \\ U \\ V \end{pmatrix} = \begin{pmatrix} I_h + I_v \\ I_h - I_v \\ I_{45^\circ} - I_{135^\circ} \\ I_R - I_L \end{pmatrix} = \begin{pmatrix} E_x^* E_x + E_y^* E_y \\ E_x^* E_x - E_y^* E_y \\ 2Re(E_x^* E_y) \\ 2Im(E_x^* E_y) \end{pmatrix},$$

where I, Q, U, V are the Stokes vector elements, I_h is the intensity of the light which would pass through a horizontal polarizer, I_v is the intensity of the light which would pass through a vertical polarizer, I_{45° is the intensity of the light which would pass through a 45° polarizer, I_{135° is the intensity of the light which would pass through a 135° polarizer, I_R is the intensity of light which would pass through a right circular polarizer, and I_L is the intensity which would pass through a left circular polarizer.

The pupil-averaged stokes vector is

$$<\vec{S}>_{pupil} = \left\langle \begin{pmatrix} E_x^* E_x + E_y^* E_y \\ E_x^* E_x - E_y^* E_y \\ 2Re(E_x^* E_y) \\ 2Im(E_x^* E_y) \end{pmatrix} \right\rangle_{pupil} = \begin{pmatrix} <E_x^* E_x + E_y^* E_y>_{pupil} \\ <E_x^* E_x - E_y^* E_y>_{pupil} \\ <2Re(E_x^* E_y)>_{pupil} \\ <2Im(E_x^* E_y)>_{pupil} \end{pmatrix} = \begin{pmatrix} <E_x^* E_x>_{pupil} + <E_y^* E_y>_{pupil} \\ <E_x^* E_x>_{pupil} - <E_y^* E_y>_{pupil} \\ 2Re(<E_x^* E_y>_{pupil}) \\ 2Im(<E_x^* E_y>_{pupil}) \end{pmatrix},$$

where the brackets represent

$<f>_{pupil} = \int f \, d\vec{\rho}$,

where $\vec{\rho}$ is the pupil coordinate. The units are chosen such that the area of the pupil is unity. $E_x^* E_x$ is the intensity of the x-polarized light in the exit pupil. Since there are no optical elements between the exit pupil and the image, there will be the same amount of x-polarized light in the image plane. Therefore,

$$\langle E_x^* E_x \rangle_{pupil} = \langle E'^*_x E'_x \rangle_{psf},$$

where the primed quantities refer to the quantities in the image plane. Clearly, the same relationship holds true for the y-polarized light:

$$\langle E_y^* E_y \rangle_{pupil} = \langle E'^*_y E'_y \rangle_{psf}.$$

Since there is the same amount of light polarized both horizontally and vertically in the exit pupil and in the image, the average of the first two elements in the Stokes vector are equal in the pupil and the point spread function,

$$\langle I \rangle_{pupil} = \langle I \rangle_{psf}$$

$$\langle Q \rangle_{pupil} = \langle Q \rangle_{psf}$$

Since the choice of horizontal and vertical is arbitrary, the same relationship holds true for the third element in the Stokes vector,

$$\langle U \rangle_{pupil} = \langle U \rangle_{psf}.$$

Since the first three elements of the Stokes vector are equal, the fourth must be equal as well,

$$\langle V \rangle_{pupil} = \langle V \rangle_{psf}.$$

These equalities can also be derived rigorously using properties of the Fourier transform. The relationship between the Jones vector in the pupil plane, $\vec{E}$, and the Jones vector in the image plane, $\vec{E}'$, is a Fourier transform,

$$\vec{E}' = \int \vec{E} e^{\iota 2\pi \vec{n}\cdot\vec{\rho}} d\vec{\rho}$$

Instead of explicitly using the x- and y- components of the electric field, we will derive the more general case, for $E_\alpha^* E_\beta$, where both α and β can be either x or y. Multiplying the Fourier transform for both components of the electric field yields

$$E'^*_\alpha E'_\beta = \int E^*_\alpha e^{-\iota 2\pi \vec{n}\cdot\vec{\rho}} d\vec{\rho} \int E_\beta e^{\iota 2\pi \vec{n}\cdot\vec{\rho}'} d\vec{\rho}'$$

$$= \int\int E^*_\alpha E_\beta e^{\iota 2\pi \vec{n}\cdot(\vec{\rho}'-\vec{\rho})} d\vec{\rho}\, d\vec{\rho}'$$

Averaging over the point spread function yields

$$<E'^{*}_{\alpha}E'_{\beta}>_{psf} = \int E'^{*}_{\alpha}E'_{\beta}d\vec{h}$$

$$= \int\int\int E^{*}_{\alpha}E_{\beta}e^{i2\pi\vec{h}\cdot(\vec{\rho}'-\vec{\rho})}d\vec{\rho}\,d\vec{\rho}'\,d\vec{h}$$

Rearranging the order of integration yields

$$<E'^{*}_{\alpha}E'_{\beta}>_{psf} = \int\int\int E^{*}_{\alpha}E_{\beta}e^{i2\pi\vec{h}\cdot\vec{\rho}'}d\vec{\rho}'\,e^{-i2\pi\vec{h}\cdot\vec{\rho}}d\vec{h}\,d\vec{\rho}$$

$$= \int \mathcal{F}^{-1}\{\mathcal{F}\{E^{*}_{\alpha}E_{\beta}\}\}d\vec{\rho}$$

$$= \int E^{*}_{\alpha}E_{\beta}d\vec{\rho}$$

$$= <E^{*}_{\alpha}E_{\beta}>_{pupil}.$$

Therefore,

$$<E^{*}_{\alpha}E_{\beta}>_{pupil} = <E'^{*}_{\alpha}E'_{\beta}>_{psf}$$

Since α and β can both be either x or y, this proof explicitly shows that the Stokes vector averaged over the exit pupil is equal to the Stokes vector averaged over the point spread function.

Because the average Stokes vector in the point spread function is the same as the average Stokes vector in the image, the average Mueller matrix in the point spread function is the same as the average point spread function in the pupil. Qualitatively, this equality is even easier to understand than the equality for the Stokes vector. Since there are no polarizers, retarders, or depolarizers between the exit pupil and the image, the Mueller matrix for propagation from the exit pupil to the image must be the identity matrix.

This relationship can also be proven rigorously. Assuming a uniform input polarization state, we can distribute the averages among the matrices in the following way when we average over the point spread function.

$$\begin{aligned} \langle S \rangle_{PSF} &= \langle M S_{in} \rangle_{PSF} \\ &= \langle M \rangle_{PSF} S_{in} \end{aligned}.$$

A similar relationship holds when we average over the pupil.

$$\begin{aligned} \langle S \rangle_{pupil} &= \langle M S_{in} \rangle_{pupil} \\ &= \langle M \rangle_{pupil} S_{in} \end{aligned}.$$

Since we have already proven that the Stokes vector averaged over the pupil is equal to the Stokes vector over the point spread function ($\langle S \rangle_{pupil} = \langle S \rangle_{PSF}$), we can equate the previous two equations

$$\langle M \rangle_{PSF} S_{in} = \langle S \rangle_{PSF} = \langle S \rangle_{pupil} = \langle M \rangle_{pupil} S_{in}.$$

Therefore, the Mueller matrix averaged over the point spread function is equal to the Mueller matrix averaged over the exit pupil,

$$\langle M \rangle_{PSF} = \langle M \rangle_{pupil}.$$

The easiest way to find the pupil-averaged Mueller matrix, $\overline{M}(h)$, is to begin with the polarization aberration Jones matrix, $J(\rho, \phi, h)$. This matrix will have different forms depending on the symmetries of the system. To convert this Jones matrix into a Mueller matrix, use the following relationships:

$$2M_{11}(\rho,\phi,h) = J_{11}^{*}J_{11} + J_{21}^{*}J_{21} + J_{12}^{*}J_{12} + J_{22}^{*}J_{22}$$

$$2M_{12}(\rho,\phi,h) = J_{11}^{*}J_{11} + J_{21}^{*}J_{21} - J_{12}^{*}J_{12} - J_{22}^{*}J_{22}$$

$$2M_{13}(\rho,\phi,h) = J_{11}^{*}J_{12} + J_{21}^{*}J_{22} + J_{12}^{*}J_{11} + J_{22}^{*}J_{21}$$

$$2M_{14}(\rho,\phi,h) = j(J_{11}^{*}J_{12} + J_{21}^{*}J_{22} - J_{12}^{*}J_{11} - J_{22}^{*}J_{21})$$

$$2M_{21}(\rho,\phi,h) = J_{11}^{*}J_{11} + J_{12}^{*}J_{12} - J_{21}^{*}J_{21} - J_{22}^{*}J_{22}$$

$$2M_{22}(\rho,\phi,h) = J_{11}^{*}J_{11} + J_{22}^{*}J_{22} - J_{21}^{*}J_{21} - J_{12}^{*}J_{12}$$

$$2M_{23}(\rho,\phi,h) = J_{12}^{*}J_{11} + J_{11}^{*}J_{12} - J_{22}^{*}J_{21} - J_{21}^{*}J_{22}$$

$$2M_{24}(\rho,\phi,h) = j(J_{11}^{*}J_{12} + J_{22}^{*}J_{21} - J_{21}^{*}J_{22} - J_{11}^{*}J_{12})$$

$$2M_{31}(\rho,\phi,h) = J_{11}^{*}J_{21} + J_{21}^{*}J_{11} + J_{12}^{*}J_{22} + J_{22}^{*}J_{12}$$

$$2M_{32}(\rho,\phi,h) = J_{11}^{*}J_{21} + J_{21}^{*}J_{11} - J_{12}^{*}J_{22} - J_{22}^{*}J_{12}$$

$$2M_{33}(\rho,\phi,h) = J_{11}^{*}J_{22} + J_{21}^{*}J_{12} + J_{12}^{*}J_{21} + J_{22}^{*}J_{11}$$

$$2M_{34}(\rho,\phi,h) = j(J_{11}^{*}J_{22} + J_{21}^{*}J_{12} - J_{12}^{*}J_{21} - J_{22}^{*}J_{11})$$

$$2M_{41}(\rho,\phi,h) = j(J_{21}^{*}J_{11} + J_{22}^{*}J_{12} - J_{11}^{*}J_{21} - J_{12}^{*}J_{22})$$

$$2M_{42}(\rho,\phi,h) = j(J_{21}^{*}J_{11} + J_{12}^{*}J_{22} - J_{11}^{*}J_{21} - J_{22}^{*}J_{12})$$

$$2M_{43}(\rho,\phi,h) = j(J_{21}^{*}J_{12} + J_{22}^{*}J_{11} - J_{11}^{*}J_{22} - J_{12}^{*}J_{21})$$

$$2M_{44}(\rho,\phi,h) = j(J_{22}^{*}J_{11} + J_{11}^{*}J_{22} - J_{12}^{*}J_{21} - J_{21}^{*}J_{12})$$

J_{rc} represents the element from row r and column c in the Jones matrix. M_{rc} represents the element from row r and column c in the Mueller matrix. This transformation from the

Jones calculus into the Mueller calculus can be found in several references: E.L. O'Neil, Introduction to Statistical Optics, (Addison Wesley, 1963), A. Gerrard and J.M. Burch, Introduction to Matrix Methods in Optics, (Wiley, 1975).

A second, more succinct, method of transforming a Jones matrix into a Mueller matrix uses the Kroneker product:

$M = U(J \otimes J^*)U^{-1}$.

U is defined as

$$U = \begin{pmatrix} 1 & 0 & 0 & 1 \\ 1 & 0 & 0 & -1 \\ 0 & 1 & 1 & 0 \\ 0 & i & -i & 0 \end{pmatrix}.$$

The Kroneker product of two 2X2 matrices is

$$\begin{pmatrix} a_1 & b_1 \\ c_1 & d_1 \end{pmatrix} \otimes \begin{pmatrix} a_2 & b_2 \\ c_2 & d_2 \end{pmatrix} = \begin{pmatrix} a_1a_2 & a_1b_2 & b_1a_2 & b_1b_2 \\ a_1c_2 & a_1d_2 & b_1c_2 & b_1d_2 \\ c_1a_2 & c_1b_2 & d_1a_2 & d_1b_2 \\ c_1c_2 & c_1d_2 & d_1c_2 & d_1d_2 \end{pmatrix}.$$

This formalism can be found in "Obtainment of the polarizing and retardation parameters of a non-depolarizing optical system from the polar decomposition of its Mueller matrix," J. Gil, E. Bernabeu, Optik, vol. 76, no. 2, 1987.

Converting the polarization aberration Jones matrix into a Mueller matrix yields a matrix which is too complicated to even write down. However, by looking at the resulting Mueller matrix for the various aberration terms, we can see the form of the entire Mueller matrix. In the following analysis, we will use the polarization aberration expansion for a

rotationally symmetric system. The results from other types of systems, such as a Cassegrain telescope with an articulating secondary mirror, can be inferred from our results. We choose not to work with the polarization aberration expansion for a decentered system because the math becomes so unwieldy that the benefits of the added generality are more than outweighed by the difficulties of the added complexity. The polarization aberration expansion which we will begin with is the Jones matrix for rotationally symmetric systems:

$$J(\rho,\phi,h) = P_{0000}\sigma_0 + P_{1200}\sigma_1 h^2$$
$$P_{1111} h\rho(\cos\phi\sigma_1 - \sin\phi\sigma_2)$$
$$P_{1022}\rho^2(\cos 2\phi\sigma_1 - \sin 2\phi\sigma_2),$$

The polarization aberration terms have both real and imaginary parts

$$P_{1xxx} = r_{1xxx} + iq_{1xxx}$$

The Mueller matrix for a system with only polarization defocus is

$$\begin{pmatrix} P_{0000}^2 + P_{1022}^2\rho^4 & 2P_{0000}r_{1022}\rho^2\cos 2\phi & -2P_{0000}r_{1022}\rho^2\sin 2\phi & 0 \\ 2P_{0000}r_{1022}\rho^2\cos 2\phi & P_{0000}^2 + P_{1022}^2\rho^4\cos 4\phi & P_{1022}^2\rho^4\sin 4\phi & -2P_{0000}q_{1022}\rho^2\sin 2\phi \\ -2P_{0000}r_{1022}\rho^2\sin 2\phi & -P_{1022}^2\rho^4\sin 4\phi & P_{0000}^2 - P_{1022}^2\rho^4\cos 4\phi & -2P_{0000}q_{1022}\rho^2\cos 2\phi \\ 0 & 2P_{0000}q_{1022}\rho^2\sin 2\phi & 2P_{0000}q_{1022}\rho^2\cos 2\phi & P_{0000}^2 - P_{1022}^2\rho^4 \end{pmatrix}.$$

As expected, this is the Mueller matrix for a retarder and diattenuator with orientation that rotates at twice the angular pupil coordinate. The Mueller matrix for a system with only polarization tilt is

$$\begin{pmatrix} P_{0000}^2 + P_{1111}h^2\rho^2 & 2P_{0000}r_{1111}h\rho\cos\phi & -2P_{0000}r_{1111}h\rho\sin\phi & 0 \\ 2P_{0000}r_{1111}h\rho\cos\phi & P_{0000} + P_{1111}h^2\rho^2\cos 2\phi & -P_{1111}^2h^2\rho^2\sin 2\phi & -2P_{0000}q_{1111}h\rho\sin\phi \\ -2P_{0000}r_{1111}h\rho\sin\phi & -P_{1111}^2h^2\rho^2\sin 2\phi & P_{0000}^2 - P_{1111}^2h^2\rho^2\cos 2\phi & -2P_{0000}q_{1111}h\rho\cos\phi \\ 0 & 2P_{0000}q_{1111}h\rho\sin\phi & 2P_{0000}q_{1111}h\rho\cos\phi & P_{0000}^2 + P_{1111}h^2\rho^2 \end{pmatrix}.$$

As expected, this is the Mueller matrix for a retarder and diattenuator oriented radially. The Mueller matrix for a system with only polarization piston is

$$M_{piston} = \begin{pmatrix} P_{0000}^2 + h^4P_{1200}^2 & 2h^2P_{0000}r_{1200} & 0 & 0 \\ 2h^2P_{0000}r_{1200} & P_{0000}^2 + h^4P_{1200}^2 & 0 & 0 \\ 0 & 0 & P_{0000}^2 - h^4P_{1200}^2 & -2h^2P_{0000}q_{1200} \\ 0 & 0 & 2h^2P_{0000}q_{1200} & P_{0000}^2 - h^4P_{1200}^2 \end{pmatrix}.$$

As expected, this is the Mueller matrix for a vertical or horizontal diattenuator and retarder.

Integrate over ρ and ϕ to obtain the pupil-averaged Mueller matrix.

$$\overline{M}(h) = \int_0^1 \int_0^{2\pi} M(\rho, \phi, H)\rho\, d\rho\, d\phi$$

For rotationally symmetric systems, the pupil-averaged Mueller matrix is

$$= \begin{pmatrix} P_{0000}^2 + \frac{1}{3}P_{1022}^2 + \frac{1}{2}h^2P_{1111}^2 + h^4P_{1200}^2 & 2h^2P_{0000}r_{1200} & 0 & 0 \\ 2h^2P_{0000}r_{1200} & P_{0000}^2 + h^4P_{1200}^2 & 0 & 0 \\ 0 & 0 & P_{0000}^2 - h^4P_{1200}^2 & -2h^2P_{0000}q_{1200} \\ 0 & 0 & 2h^2P_{0000}q_{1200} & P_{0000}^2 - \frac{1}{3}P_{1022}^2 - \frac{1}{2}h^2P_{1111}^2 - h^4P_{1200}^2 \end{pmatrix} \quad 1$$

$$\cong \begin{pmatrix} P_{0000}^2 & 2h^2 P_{0000} r_{1200} & 0 & 0 \\ 2h^2 P_{0000} r_{1200} & P_{0000}^2 & 0 & 0 \\ 0 & 0 & P_{0000}^2 & -2h^2 P_{0000} q_{1200} \\ 0 & 0 & 2h^2 P_{0000} q_{1200} & P_{0000}^2 \end{pmatrix} \qquad 2$$

This is the Mueller matrix which would be measured in the image plane if the system were placed in a polarimeter. The approximation in eq. 2 is the usual approximation used in aberration theory; terms of high order in h and terms on the order P_{1xxx}^2 are neglected. Making this approximation has a slight drawback; the resulting Mueller matrix is slightly unphysical. If linearly polarized light at 45° is incident on the Mueller matrix,

$$S_{in} = \begin{pmatrix} 1 \\ 0 \\ 1 \\ 0 \end{pmatrix},$$

the pupil-average stokes vector is

$$S_{out} = \begin{pmatrix} P_{0000}^2 \\ 2h^2 P_{0000} r_{1200} \\ P_{0000}^2 \\ 2h^2 P_{0000} q_{1200} \end{pmatrix}.$$

The degree of polarization for this Stokes vector is

$$\text{DOP} = \sqrt{Q^2 + U^2 + V^2}/I$$
$$\cong 1 + 2h^4 P_{1200}^2 .$$

This Stokes vector is unphysical because the degree of polarization is greater than one.

This is not a serious problem, however, because, to be consistent with our previous approximations, we should drop terms of order P^2_{1xxx}. In this case, the degree of polarization for this Stokes vector is unity,

$\mathrm{DOP} \cong 1$.

Now that we have a pupil-averaged Mueller matrix, we can rigorously define the three polarization aberration criteria which we enumerated in Section II.

Polarization error #1 was that unpolarized light should not couple into polarized light. The Stokes vector for unpolarized light is

$$S = \begin{pmatrix} 1 \\ 0 \\ 0 \\ 0 \end{pmatrix}.$$

When this unpolarized light is incident on the system, she Stokes vector averaged over the exit pupil is

$$S = \begin{pmatrix} P^2_{0000} \\ 2h^2 P_{0000} \Gamma_{1200} \\ 0 \\ 0 \end{pmatrix}.$$

This is the polarization error which we believe is the most important, and should be kept below 10^{-5}. Since P_{0000}, the transmission for the system, is approximately equal to one, the polarization specification for this system should be

$2r_{1200} < 10^{-5}$.
This is the polarization specification which we recommend. This specification is essentially a limit on the diattenuation along the chief ray.

Polarization error #2 is that polarized light should maintain its polarization state. This specification would limit all off-diagonal elements in the pupil-averaged Mueller matrix. One way to quantify this specification would be
$2|P_{1200}| < 10^{-5}$.
This specification is essentially a limit on the diattenuation and retardance along the chief ray path. We do not recommend this specification because we believe that it is too stringent. Furthermore, all of the typical, low diattenuation coatings which we have analyzed have low retardance as well. Therefore, any set of coatings which would meet the first specification would also have a small value for the second specification.

Polarization error #3 is that polarized light should not couple into unpolarized light. Determining the amount of depolarization in a Mueller matrix is an active area of research, but we can determine some properties of the pupil-averaged Mueller matrix by examining the Mueller matrix in eq. 1 on a term-by-term basis. For a system with only polarization defocus, the pupil-averaged Mueller matrix is

$$M_{defocus} = \begin{pmatrix} P^2_{0000} + \frac{1}{3}P^2_{1022} & 0 & 0 & 0 \\ 0 & P^2_{0000} & 0 & 0 \\ 0 & 0 & P^2_{0000} & 0 \\ 0 & 0 & 0 & P^2_{0000} - \frac{1}{3}P^2_{1022} \end{pmatrix}.$$

For a system with only polarization tilt, the pupil-averaged Mueller matrix is

$$M_{tilt} = \begin{pmatrix} P_{0000}^2 + \frac{1}{2}h^2 P_{1111}^2 & 0 & 0 & 0 \\ 0 & P_{0000}^2 & 0 & 0 \\ 0 & 0 & P_{0000}^2 & 0 \\ 0 & 0 & 0 & P_{0000}^2 - \frac{1}{2}h^2 P_{1111}^2 \end{pmatrix}.$$

The pupil-averaged Mueller matrices for a system with only tilt or with only defocus is the Mueller matrix for a depolarizer. The first element in the Stokes vector will be increased, but the other three will remain the same or decrease. For a system with only polarization piston, the pupil-averaged Mueller matrix is

$$M_{piston} = \begin{pmatrix} P_{0000}^2 + h^4 P_{1200}^2 & 2h^2 P_{0000} r_{1200} & 0 & 0 \\ 2h^2 P_{0000} r_{1200} & P_{0000}^2 + h^4 P_{1200}^2 & 0 & 0 \\ 0 & 0 & P_{0000}^2 - h^4 P_{1200}^2 & 2h^2 P_{0000} q_{1200} \\ 0 & 0 & -2h^2 P_{0000} q_{1200} & P_{0000}^2 - h^4 P_{1200}^2 \end{pmatrix}.$$

The defocus term and the tilt term are clearly depolarizers. The piston term, perhaps not so clearly, is a diattenuator and a retarder. The depolarization of the entire Mueller matrix is

$D = \frac{1}{3}P_{1022}^2 + \frac{1}{2}h^2 P_{1111}^2$

This depolarization is clearly a small effect; all of the aberration terms are on the order of P_{1xxx}^2.

For slightly decentered systems, such as a Cassegrain telescope with a tilted secondary mirror, the polarization aberration expansion in Jones matrix form becomes

much longer, and the corresponding pupil-averaged Mueller matrix becomes correspondingly larger. Rather than writing the equations, it is more instructive to think through the problem.

The Mueller matrix in eq. 2 is the Mueller matrix which represents a diattenuator. The magnitude of the diattenuation increases quadratically from the center of the field to the edge. For the Mueller matrix for the decentered system will look much more complicated, but the meaning will be very similar. The orientation of the diattenuation will be oriented radially about some non-axial image point, and the magnitude of the diattenuation will increase quadratically from the same, non axial image point. Therefore, we specified the coatings to meet the 10^{-5} polarization specification at the most extreme point in the image plane with a tilted secondary mirror.